An Analytical Method to Implement High Sensitivity Transmission Line Differential Sensors for Dielectric Constant Measurements

Jonathan Muñoz-Enano, *Graduate Student Member, IEEE*, Paris Vélez, *Member, IEEE*, Marta Gil, and Ferran Martín, *Fellow, IEEE*

Abstract— **A simple analytical method useful to optimize the sensitivity in differential sensors based on a pair of meandered microstrip lines is presented in this paper. Sensing is based on the phase difference of the transmission coefficients of both lines, when such lines are asymmetrically loaded. The analysis provides the combination of operating frequency and line length (the main design parameters) that are necessary to obtain the maximum possible differential phase (±180º) for a given level of the differential dielectric constant (input dynamic range). The proposed sensor is useful to detect tiny defects of a sample under test (SUT) as compared to a reference (REF) sample. It can also be applied to the measurement of the complex dielectric constant of the SUT, where the real part is inferred from the differential phase, whereas the imaginary part, or the loss tangent, is derived from the modulus of the transmission coefficient of the line loaded with the SUT. It is experimentally demonstrated that the proposed device is able to detect the presence of few and small (purposely generated) defects in a commercial microwave substrate, as well as subtle variations in their density, pointing out the high achieved sensor sensitivity. Sensor validation is also carried out by determining the dielectric constant and loss tangent of commercial microwave substrates.**

Index Terms — **Dielectric characterization, differential sensors, microstrip, microwave sensors.**

I. INTRODUCTION

THERE are many approaches for the dielectric characterization of solids and liquids using microwaves. Among the methods that use transmission line based structures, an extended sensing principle is based on the variation of the resonance frequency and notch/peak magnitude of a resonator-loaded line, caused by loading the sensitive part of the resonator with the sample under test (SUT) [1]-[8]. These sensors are simple but they are subjected to potential cross sensitivities related to changes in environmental factors (e.g., temperature or humidity). By contrast, sensors based on symmetry disruption are robust against such cross-sensitivities [9],[10]. The reason is that, in these symmetry-based sensors, variations in ambient conditions are seen as common mode stimulus, unable to generate an appreciable response in the sensor.

Coupling modulation [11]-[19], frequency splitting [20]-[26] and differential sensors [27]-[30] belong to the category of microwave sensors based on symmetry properties. Differential sensors consist of two independent sensing elements, and the output variable is generated in response to a differential input variable, e.g., the difference in the dielectric constant of a reference sample (REF) and the SUT. In frequency splitting sensors, a single transmission line based sensor is used, but it is equipped with two independent sensitive elements (resonators) symmetrically loading the line. In this case, the measurand is also a differential magnitude. By contrast, coupling modulation sensors are based on a single sensor structure and a unique sensitive element (a symmetric resonator symmetrically loading the line). Thus, this later type of sensors is not appropriate for differential sensing (most reported coupling modulation sensors have been applied to the measurement of linear and angular displacements and velocities [11]-[19]).

Many differential sensors devoted to dielectric characterization of solids and liquids are based on resonator loaded lines (like frequency splitting sensors). Examples are the sensors reported in [29],[30], able to detect tiny concentrations of electrolytes in deionized (DI) water, or variations in the composition of liquids, as compared to a reference, caused by the difference in the permittivity [29]. In such sensors, the output variable is the cross-mode transmission coefficient, whose magnitude is dictated by the level of asymmetry (in turn given by the input differential variable).

The resolution and sensitivity of the resonator-based differential sensors reported in [29],[30] for the measurement of the electrolyte concentration in aqueous solutions are good. This is attributed to the fact that the loss tangent of water is very sensitive to changes in the electrolyte content. Therefore appreciable variations in the magnitude of the resonance, related to changes in the electrolyte concentration, are caused in the SUT sensing line (as compared to the REF line), thereby

providing significant variations in the cross mode transmission coefficient. Despite the fact that electrolyte concentrations as small as 0.25 g/L have been resolved [29], and sensitivities as high as 12.27 dB/(g/L) have been experimentally demonstrated [30], the output dynamic range of the sensors is limited. Moreover, the resonator-based differential sensors exhibit a limited resolution and sensitivity in regard to liquid composition, mainly related to the dielectric constant.

In this paper, differential sensors, based on a pair of meandered lines, for the measurement of differential dielectric constants are proposed. Moreover, an analytical method, useful for sensor design on the basis of the required sensitivity and input dynamic range, is presented. Application of this method provides a sensor with extremely high (adjustable) sensitivity, able to detect tiny changes in material composition and defects. The proposed sensing method is similar to the one reported in [28]. The novelty of the paper concerns the fact that from the reported analysis, the length of the meander lines (given the operational frequency) that is needed in order to obtain the required sensor sensitivity, is provided. Moreover, the paper demonstrates that not only the differential dielectric constant can be obtained (from which the dielectric constant of the SUT is inferred), but also the loss tangent of the SUT can be obtained from the response of the SUT line. Additionally, the sensor can be useful as comparator, able to detect tiny differences between the REF and the SUT samples, thanks to the high sensitivity of the structure as differential mode sensor.

II. Sensing principle and analysis

The sensing principle of the proposed differential sensor is the variation of the electrical length of the sensing line, as compared to the reference line, when such lines are loaded with the SUT and REF samples, respectively. The considered lines are meandered microstrip lines, with a phase velocity that depends on the dielectric constant of the surrounding material. Therefore, the differential dielectric constant, $\Delta\varepsilon = \varepsilon_{REF} - \varepsilon_{SUT}$ (where ε_{REF} and ε_{SUT} are the dielectric constants of the REF and SUT samples, respectively), will determine the differential phase, $\Delta\phi = \phi_{REF} - \phi_{SUT}$ (where ϕ_{REF} and ϕ_{SUT} are the electrical lengths of the REF and SUT line, respectively). In order to express $\Delta\phi$ in terms of $\Delta\varepsilon$, let us first write the differential phase as a function of the effective dielectric constants of the REF line, $\varepsilon_{eff,REF}$, and SUT line, $\varepsilon_{eff,SUT}$, i.e.,

$$\Delta\phi = \beta_0 l\left(\sqrt{\varepsilon_{eff,REF}} - \sqrt{\varepsilon_{eff,SUT}}\right) \tag{1}$$

where l is the length of the meandered lines, and $\beta_0 = \omega/c$ is the phase constant in vacuum, ω and c being the angular frequency and the speed of light in vacuum, respectively.

Let us now assume that the REF and SUT samples, in contact with the sensor lines, are thick enough, so as to consider them as semi-infinite in the transverse direction to the plane of the lines. Under this approximation, the effective dielectric constant of the REF line can be expressed as [31]

$$\varepsilon_{eff,REF} = \frac{\varepsilon_{SUB} + \varepsilon_{REF}}{2} + \frac{\varepsilon_{SUB} - \varepsilon_{REF}}{2}F \tag{2}$$

where ε_{SUB} is the dielectric constant of the substrate, and F is a function of the line geometry given by

$$F = \left(1 + 12\frac{h}{W}\right)^{-1/2} \tag{3}$$

In (2) and (3), it has been assumed that the thickness of the line strip is negligible (as compared to substrate thickness, h), and that the width of the line, W, is larger than h. The effective dielectric constant for the SUT line is also given by (2), by simply replacing ε_{REF} with ε_{SUT}. Expression (2) is obtained from the formula of the effective dielectric constant of a microstrip line (covered by air), as detailed in [31], but replacing the dielectric constant of air ($\varepsilon_r = 1$) with the dielectric constant of the REF sample (ε_{REF}).

Introducing the effective dielectric constants of both lines in (1), one obtains

$$\Delta\phi = \frac{\beta_0 l}{\sqrt{2}}\left(\sqrt{\varepsilon_{SUB}(1+F) + \varepsilon_{REF}(1-F)} - \sqrt{\varepsilon_{SUB}(1+F) + \varepsilon_{SUT}(1-F)}\right) \tag{4}$$

and assuming that $\Delta\varepsilon \ll \varepsilon_{REF}$, expression (4) can be approximated by

$$\Delta\phi = \frac{\beta_0 l}{2\sqrt{2}} \frac{\Delta\varepsilon(1-F)}{\sqrt{\varepsilon_{SUB}(1+F) + \varepsilon_{REF}(1-F)}} \tag{5}$$

Note that the interest in this paper is to obtain very good sensor resolution and sensitivity, in order to discriminate and measure small differential dielectric constants. For this reason, the above-cited approximation is justified. However, the sensor can be also designed to measure larger input dynamic ranges (differential dielectric constants), at the expense of a degradation in the sensitivity (considering the same output dynamic range, between +180° and -180°).

III. Sensor design and fabrication

In order to optimize sensor sensitivity, the output dynamic range must be (ideally) $\Delta\phi_{max} = \pm\pi$, for differential dielectric constants varying within a range delimited by a certain maximum value, $\Delta\varepsilon = \pm\Delta\varepsilon_{max}$, $\Delta\varepsilon_{max}$ being a design specification. Introducing these values in (5) and isolating $\beta_0 l$, the following result is obtained

$$\beta_0 l = 2\sqrt{2}\pi \frac{\sqrt{\varepsilon_{SUB}(1+F) + \varepsilon_{REF}(1-F)}}{\Delta\varepsilon_{max}(1-F)} \tag{6}$$

From the geometry of the line (W), substrate parameters (ε_{SUB}, h), dielectric constant of the REF sample, ε_{REF}, and $\Delta\varepsilon_{max}$, equation (6) provides the single design parameter of the sensor, i.e., $\beta_0 l$. For small values of $\Delta\varepsilon_{max}$, the case of interest, either a high operating frequency or long lines are necessary in order to optimize the sensitivity. Since operation at high frequencies may increase the cost of the sensor in a real scenario, it is convenient to assume the need of long lines, which can be meandered in order to obtain a reasonable shape factor of the sensitive area of the sensor. Nevertheless, inspection of (6) reveals that considering substrates with small dielectric constant, ε_{SUB}, helps in reducing the length of the lines (this also applies to ε_{REF}, but this parameter is not a design variable).

The considered sensor substrate is the *Rogers RO4003C* with dielectric constant $\varepsilon_{SUB} = 3.5$, thickness $h = 0.8128$ mm

and loss tangent $\tan\delta_{SUB} = 0.0027$. The REF sample is considered to exhibit the characteristics of the *Nelco N4350-13RF* substrate, with dielectric constant $\varepsilon_{REF} = 3.55$, and dissipation factor $\tan\delta_{REF} = 0.0065$ (a semi-infinite sample in the vertical direction has been considered). With these material properties, the width of the REF line necessary to provide a 50-Ω characteristic impedance is found to be $W = 1.6$ mm. Let us consider that the measurement range of the dielectric constant of the SUT sample corresponds to a differential dielectric constant of $\Delta\varepsilon_{max} = 0.45$, i.e., limited to 12.7 % variations of the dielectric constant of the REF sample. Evaluation of (5) gives $\beta_0 l = 84.23$ rad. By considering an operating frequency of $f_0 = \omega/2\pi = 6$ GHz, the length of the meandered lines is found to be $l = 670.3$ mm. Such long line length line is the reason for line meandering, but similar results are achievable by using straight lines (obviously, with the penalty of an excessive sensor dimension in the direction of the line axis).
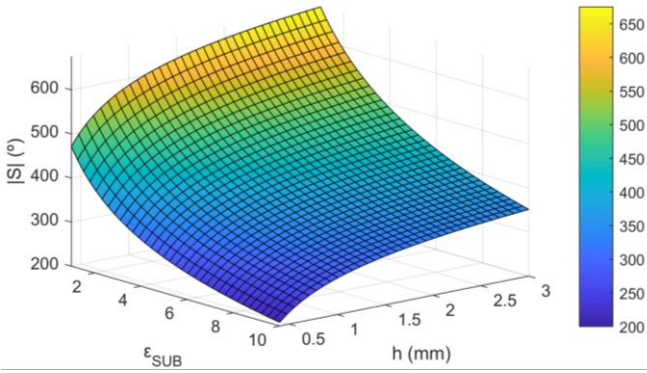

Fig. 1. 3D plot showing the dependence of the sensitivity on the dielectric constant and thickness of the substrate, as derived from expression (5).The necessary parameters for the calculation of *S* from (5) are given in the text.

Interestingly, according to (5), a small value of the dielectric constant of the substrate, ε_{SUB}, is convenient for sensitivity optimization (for a fixed value of $\beta_0 l$). Concerning substrate thickness, h, increasing h has the effect of decreasing F (expression 3), and this, in turn, has the effect of enhancing the sensitivity. Figure 1 depicts the dependence of the sensitivity ($S = d\Delta\phi/d\Delta\varepsilon$) as inferred from the approximate expression (5), as a function of both the dielectric constant, ε_{SUB}, and thickness, h, of the substrate. It should be clarified, however, that if $\beta_0 l$ is determined from (6), the sensitivity is $S = d\Delta\phi/d\Delta\varepsilon = \Delta\phi_{max}/\Delta\varepsilon_{max}$ regardless of h and ε_{SUB}. But note that the resulting $\beta_0 l$ value increases with ε_{SUB} and decreases with h. For these reasons we have selected the considered sensor substrate, with relatively small dielectric constant and relatively thick dielectric layer. Thus, the proposed design procedure of the sensor allows us to set the sensitivity to a required value, and the resulting line length is determined by the substrate characteristics. The plot of Fig. 1, corresponding to a fixed value of $\beta_0 l$, i.e., the nominal value given by (6), must be understood as the tolerance of the sensitivity against changes in the dielectric constant and thickness of the substrate.

Figure 2(a) depicts the photograph of the bare sensor with relevant dimensions indicated (the sensor has been fabricated

by means of the *LPKF H100* drilling machine), whereas the sensor loaded with the REF and SUT samples is depicted in Fig. 2(b). The lines have been meandered in order to achieve a roughly square shape factor for the sensing area (indicated in the figure). We have then obtained from full-wave electromagnetic simulation (using *Keysight Momentum*) the differential phase of the structure as a function of the dielectric constant of the SUT, by considering variations in the vicinity of $\varepsilon_{REF} = 3.55$ with $\Delta\varepsilon_{max} = 0.45$. The results, for different values of the loss tangent of the SUT, are depicted in Fig. 3. The curves are almost undistinguishable, which means that the loss factor of the SUT does not play an important role on the differential phase. Moreover, the simulated curves of Fig. 3 are in very good agreement with the analytical expression (5), also included in the figure. These results validate the analysis of the previous section, and point out that it is not necessary to know in advance the loss tangent of the SUT sample in order to determine its dielectric constant. Note that for the SUT sample with the highest or lowest dielectric constant (corresponding to $\pm\Delta\varepsilon_{max}$), $\Delta\phi = \phi_{REF} - \phi_{SUT} = \pm\pi$. The sensitivity, roughly constant, has been found to be $S = d\Delta\phi/d\Delta\varepsilon = -415.6°$ (very close to the theoretical value, i.e., $-400°$) and the sensor is able to detect extremely small differential dielectric constants.

For the determination of the loss tangent of the SUT, the output variable can be the magnitude of the transmission coefficient of the SUT line ($|S_{43}|$). Figure 4 depicts the simulated $|S_{43}|$ at f_0 as a function of the dielectric constant, by considering the loss tangent of the SUT as a parameter. It can be appreciated that the dependence of $|S_{43}|$ on the dielectric constant is roughly negligible. That is, $|S_{43}|$ is dictated by the loss factor of the SUT, and thereby it can be considered as the output variable for the determination of the loss tangent of the SUT.
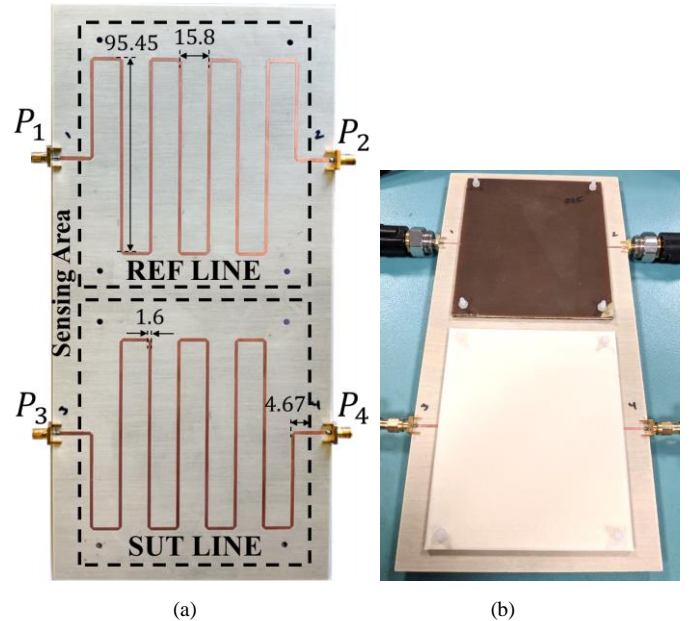

(a)　　　　　　　　(b)

Fig. 2. Photograph of the designed differential sensor without (a) and with (b) REF and SUT samples on top of it (dimensions are given in mm).
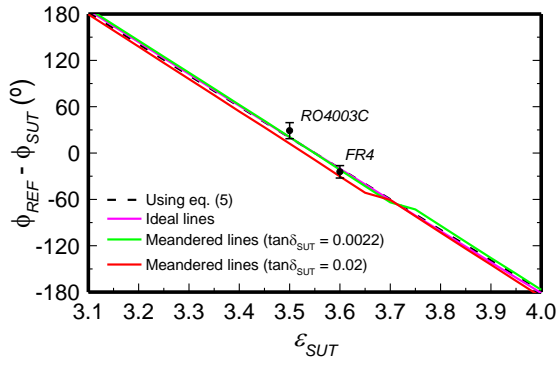
Fig. 3. Simulated differential phase at $f_0 = 6$ GHz of the proposed sensor as a function of the dielectric constant of the SUT, parameterized by the loss tangent of the SUT. The curve given by expression (5) is also included. The mean of the measured differential phases (with $N = 3$ independent measurements) for the indicated materials, as well as the error bars inferred from the standard deviation, are also included.
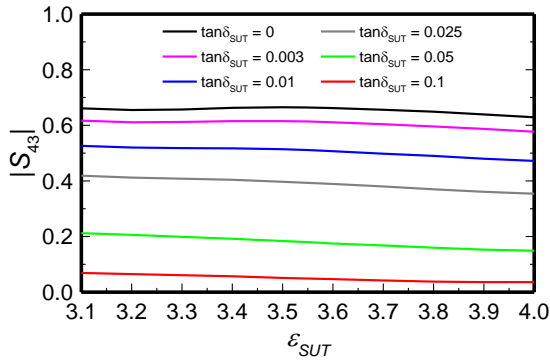

Fig. 4. Simulated transmission coefficient of the SUT line at $f_0 = 6$ GHz, as a function of the dielectric constant of the SUT, for different values of the loss tangent of the SUT.

IV. EXPERIMENTAL VALIDATION

Experimental validation has been first carried out by loading the sensing region with a commercial microwave substrate with well-known dielectric constant, i.e., the *FR4* substrate with $\varepsilon_{SUT} = 4.5$. The thickness of the REF sample is 3.3 mm, whereas the one of the SUT is 3.2 mm (achieved by stacking two samples). With these thicknesses, the samples can be roughly considered to be semi-infinite. Namely, the electromagnetic field generated by the lines do not reach the REF/air (or SUT/air) interface (under these conditions, the analysis of Section II is valid). This aspect has been corroborated by means of simulations, not included in the paper, which demonstrate that 3 mm is a sufficient sample thickness (for thicker samples, the phase of the lines does not experience an appreciable variation).

Note that ε_{SUT} (or $\Delta\varepsilon$) is out of the considered input dynamic range. However, the measured differential phase, $\Delta\phi$, is a periodic function with $\Delta\varepsilon$ (actually, $\Delta\phi$ varies linearly with $\Delta\varepsilon$, but any measured value of $\Delta\phi$ out of the range $[-\pi, +\pi]$ is expressed by its equivalent value within that range). Thus, from the measured differential phase, it is possible to check the validity of the approach (the limitation is dictated by the requirement $\Delta\varepsilon << \varepsilon_{REF}$). According to the results of Fig. 3, the expected value of the differential phase for $\varepsilon_{SUT} = 4.5$ is $\Delta\phi = -19.18º$ (equivalent to $\varepsilon_{SUT} = 3.6$), whereas the mean of the measured values at 6 GHz ($N = 3$ independent

measurement have been carried out) is $\Delta\phi = -24.23º$ (Fig. 5), i.e., in very good agreement, taking into account the relatively large value of ε_{SUT}. We have also carried out the experiment by considering as SUT a piece of *Rogers RO4003C* substrate with $\varepsilon_{SUT} = 3.5$ (satisfying $\Delta\varepsilon << \varepsilon_{REF}$) and thickness 3.05 mm (also achieved by stacking two samples). The resulting mean of the measured differential phases at 6 GHz (also with $N = 3$ independent measurements) is $\Delta\phi = 28.97º$ (Fig. 5), in good agreement with the expected value ($\Delta\phi = 20.34º$). The measured differential phases at 6GHz are depicted in Fig. 3 to ease the comparison with the theoretical value. Note that from the measured phases, the dielectric constant values inferred from expression (5) for *FR4* and *RO4003C* are found to be 4.51 and 3.48, respectively, i.e., very close to the nominal values. It should be mentioned that the alignment of the REF and SUT samples is not critical as far as these samples cover the same extension in both lines, delimited by the sensing area [indicated in Fig. 2(b)]. In order to minimize the effects of the air gap (between the substrate and the REF and SUT samples), we have used Teflon screws and we have added pressure to the SUT and REF samples against the substrate.

Concerning material losses, Fig. 4 can potentially be used to determine the loss tangent from the value of the transmission coefficient (magnitude) of the SUT line. However, discrepancies between the simulated and measured transmission coefficient are inevitable due to the effects of the access lines and connectors (not accounted for in the simulations). Indeed, determining the loss tangent from analytical expressions is not feasible because of the above cited effects, and also due to meandering of the lines and metal losses. Consequently, we have measured the magnitude of the transmission coefficient for several samples with different value of the loss tangent. The obtained $|S_{43}|$ values at f_0 are depicted in Fig.6. From these values, a calibration curve can be generated (see Fig. 6, inset), and this curve is useful to determine the loss tangent of the SUT from the measured value of $|S_{43}|$. The considered samples for the generation of the calibration curve are the *FR4* and *Rogers 4003C* substrates indicated in the previous paragraph, as well as the *Nelco N4350-13RF* substrate (the REF sample for the differential phase measurements). Nevertheless, we have also measured the transmission coefficient of the unloaded SUT line (corresponding to $\tan\delta_{SUT} = 0$), as it provides an additional data point.

To validate the approach for the determination of the loss tangent, we have fabricated two samples with a 3D-printer (model *Ultimaker 3 Extended*). The loss factor of such samples, measured by means of the *Agilent Keysight 85072A* commercial resonant cavity, are $\tan\delta_{SUT} = 0.010$ (for SUT1, fabricated by considering *PLA* as filament) and $\tan\delta_{SUT} = 0.016$ (for SUT2, fabricated by considering *RS Pro MT-COPPER* as filament). The measured values of the insertion loss at f_0 that are obtained by loading the SUT line with these 3D-printed samples are indicated in Fig. 6. It can be seen that the resulting points are in reasonable agreement with the calibration curve. Therefore, it is demonstrated that such curve can be used to estimate the loss tangent of the SUT sample.
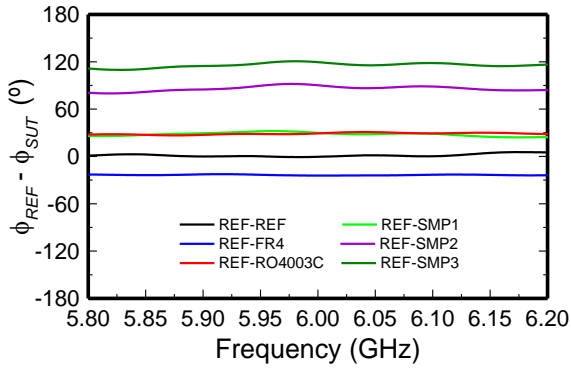
Fig. 5. Measured differential phase for different SUT samples, including *FR4* and *Rogers RO4003C* slabs, as well as samples identical to the REF sample and different densities of holes across the substrate. Measurements have been performed by means of the *Keysight N5221A* four-port vector network analyzer. For *FR4* and *RO-4003C*, the mean measured differential phase with $N = 3$ independent measurement is depicted.
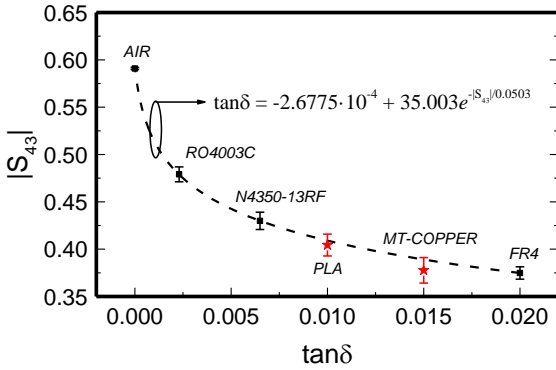

Fig. 6. Measured transmission coefficient at $f_0 = 6$ GHz for different (indicated) SUT samples. The mean values, as well as the error bars, obtained from $N = 3$ independent measurements are depicted.

Let us now demonstrate the potential of the designed structure as highly sensitive comparator, able to detect small differences between the SUT and REF samples. Due to the lack of available substrates, or materials, with small variations of the dielectric constant in the vicinity of ε_{REF}, we have emulated the differences between the REF and SUT samples by generating sparse defects (holes across the substrate) of different densities in samples identical to the REF sample (Fig. 7). The measured differential phases for such SUT samples are also included in Fig. 5. As it can be appreciated, the sensor is able to detect the presence of extremely small densities of holes in the SUT sample, pointing out the potential to detect tiny defects in the SUT sample (as compared to the REF sample).
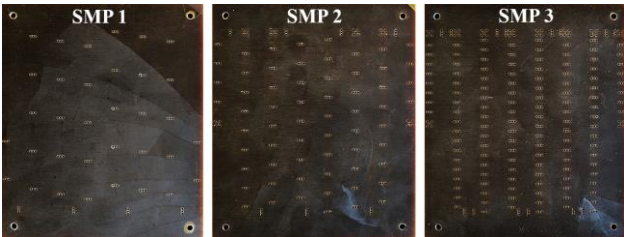

Fig. 7. Photographs of the SUT samples generated by opening hole arrays of different densities across the *Nelco N4350-13RF* substrate (the REF sample). The diameter of the holes is 1 mm, and the hole density is 0.84 holes/cm², 1.81 holes/cm², and 3.50 holes/cm² in samples SMP1, SMP2 and SMP3, respectively.

V. COMPARISON TO OTHER SENSORS

The comparison of the reported sensor in terms of sensor performance with other sensors available in the literature is not straightforward, since the working principle of most dielectric constant sensors is based on frequency variation or frequency splitting. Due to the different output variables in such sensors, a sensitivity comparison with the sensor reported in this work is not possible. The sensor reported in [28] is based on similar principle. Nevertheless, sensitivity comparison is not concluding even in this case, since the sensitivity of the proposed sensor can be made as high as required by simply increasing the length of the meander lines (as discussed before).

An advantage of the proposed sensor is that it operates at a single frequency. Moreover, due to the high sensitivity, the sensor exhibits high resolution in the determination of the differential dielectric constant. Assuming that phase differences of $\Delta\phi = 5°$ can be detected (a conservative value), it follows that the resolution is as small as 0.0120. Table I summarizes some characteristics of various sensors devoted to dielectric constant measurements, where the operating principle, the frequency span required for measurement (i.e., a single frequency or a frequency scan), the sensitivity and the resolution, are indicated. Note that the sensitivity units are not the same due to the different working principles, as mentioned. Sensor resolution is not given in most works. Nevertheless, assuming that frequency variations as small as 1 MHz can be detected in frequency variation or frequency splitting sensors (an extremely small value for sensors operating at GHz frequencies), the corresponding variation of the dielectric constant (equivalent to the resolution) can be calculated. The results are given in the Table I. It can be appreciated that the proposed sensor exhibits very competitive resolution in the measurement of the dielectric constant (note that the considered phase discrimination, $\Delta\phi = 5°$, is a conservative value, as compared to the considered frequency discrimination, 1 MHz).

TABLE I
COMPARISON OF VARIOUS SENSORS DEVOTED TO DIELECTRIC CONSTANT MEASUREMENTS

Ref.	Working principle*	Freq. span	Sensitivity	Resolution
[26]	Δf	yes	1.13 MHz	0.8849
[29]	Δf	yes	2.05 MHz	0.4878
[32]	Δf	yes	81.25 MHz	0.0123
[25]	Δf	yes	47.81 MHz	0.0210
[33]	Δf	yes	46.51 MHz	0.0215
[24]	Δf	yes	29.34 MHz	0.0341
[5]	Δf	yes	62.12 MHz	0.0161
[6]	Δf	yes	66.30 MHz	0.0151
[34]	Δf	yes	73.03 MHz	0.0137
[35]	Δf	yes	32 MHz	0.0312
[36]	Δf	yes	116.86 MHz	0.0086
[37]	Δf	yes	70.51 MHz	0.0142
[38]	Δf	yes	6.28 MHz	0.1592
[28]	$\Delta\phi$	no	54.85°	0.0911
T.W.	**$\Delta\phi$**	**no**	**415.6°**	**0.0120**

*Δf and $\Delta\phi$ stands for frequency variation and phase variation, respectively.

VI. Conclusions

In conclusion, an analytical method to implement highly sensitive differential permittivity sensors based on meandered lines has been reported and experimentally validated. In such sensor, the differential output variable is the phase balance between the pair of lines, whereas the differential dielectric constant (between the REF and SUT samples) is the considered input variable. It has been shown that for small values of the input variable, the sensitivity is roughly constant and proportional to the length of the meandered lines. Particularly, the fabricated sensor has been designed in order to exhibit a nominal sensitivity of $|S| = -400°$. It has been found that the differential phase does not depend on the loss tangent of the SUT sample. Thus, the dielectric constant of the SUT sample can be easily inferred from the measured differential phase. It has been also shown in the paper that the dielectric constant of the SUT has very small impact on the magnitude of the insertion loss of the SUT line, mainly determined by the loss tangent of the SUT sample. Therefore, such insertion loss magnitude has been used as the output variable for the determination of the loss factor of the SUT. Finally, it has been demonstrated that the designed differential sensor can be used as highly sensitive comparator, able to detect tiny defects (sparse hole arrays) in a sample, as compared to a reference one. As compared to other planar dielectric constant sensors, the reported device exhibits a good combination of sensitivity (with measured value of 415.6°) and resolution (0.0120). Moreover, as it is not based on frequency variation, wideband frequency measurements for the determination of the permittivity of the samples under test are not required.

References

[1] M. Puentes, C. Weiß, M. Schüßler, and R. Jakoby, "Sensor array based on split ring resonators for analysis of organic tissues," in *IEEE MTT-S Int. Microw. Symp.*, Baltimore, MD, USA, Jun. 2011, pp. 1–4.

[2] M. Puentes, *Planar Metamaterial Based Microwave Sensor Arrays for Biomedical Analysis and Treatment*, Springer, Heidelberg, Germany, 2014.

[3] A. Ebrahimi, W. Withayachumnankul, S. Al-Sarawi, D. Abbott, "High-sensitivity metamaterial-inspired sensor for microfluidic dielectric characterization," *IEEE Sensors J.*, vol. 14, pp. 1345−1351, May 2014.

[4] M. Schueler, C. Mandel, M. Puentes, and R. Jakoby, "Metamaterial inspired microwave sensors," *IEEE Microw. Mag.*, vol. 13, no. 2, pp. 57–68, Mar. 2012.

[5] M. S. Boybay and O. M. Ramahi, "Material characterization using complementary split-ring resonators," *IEEE Trans. Instrum. Meas.*, vol. 61, no. 11, pp. 3039−3046, Nov. 2012.

[6] C.-S. Lee and C.-L. Yang, "Complementary split-ring resonators for measuring dielectric constants and loss tangents," *IEEE Microw. Wireless Compon. Lett.*, vol. 24, no. 8, pp. 563−565, Aug. 2014.

[7] C.-L. Yang, C.-S. Lee, K.-W. Chen, and K.-Z. Chen, "Noncontact measurement of complex permittivity and thickness by using planar resonators," *IEEE Trans. Microw. Theory Techn.*, vol. 64, no.1, pp. 247−257, Jan. 2016.

[8] L. Su, J. Mata-Contreras, P. Vélez, A. Fernández-Prieto, and F. Martín, "Analytical method to estimate the complex permittivity of oil samples", *Sensors*, vol. 18, p. 984, 2018.

[9] F. Martín, *Artificial Transmission Lines for RF and Microwave Applications*, John Wiley, Hoboken, NJ, 2015.

[10] J. Naqui, *Symmetry Properties in Transmission Lines Loaded with Electrically Small Resonators*, Springer, Heidelberg, Germany, 2016.

[11] J. Naqui, M. Durán-Sindreu and F. Martín, "Novel sensors based on the symmetry properties of split ring resonators (SRRs)," *Sensors*, vol 11, pp. 7545−7553, 2011.

[12] J. Naqui, M. Durán-Sindreu, and F. Martín, "Alignment and position sensors based on split ring resonators," *Sensors*, vol. 12, pp. 11790−11797, 2012.

[13] A.K. Horestani, C. Fumeaux, S.F. Al-Sarawi, and D. Abbott, "Displacement sensor based on diamond-shaped tapered split ring resonator," *IEEE Sens. J.*, vol. 13, pp. 1153–1160, 2013.

[14] A.K. Horestani, D. Abbott, and C. Fumeaux, "Rotation sensor based on horn-shaped split ring resonator," *IEEE Sens. J.*, vol. 13, pp. 3014–3015, 2013.

[15] J. Naqui and F. Martín, "Transmission lines loaded with bisymmetric resonators and their application to angular displacement and velocity sensors," *IEEE Trans. Microw. Theory Techn.*, vol. 61, no. 12, pp. 4700–4713, Dec. 2013.

[16] J. Naqui and F. Martín, "Angular displacement and velocity sensors based on electric-LC (ELC) loaded microstrip lines," *IEEE Sensors J.*, vol. 14, no. 4, pp. 939–940, Apr. 2014.

[17] A.K. Horestani, J. Naqui, D. Abbott, C. Fumeaux, and F. Martín, "Two-dimensional displacement and alignment sensor based on reflection coefficients of open microstrip lines loaded with split ring resonators," *Elec. Lett.*, vol. 50, pp. 620–622, Apr. 2014.

[18] A. Ebrahimi, W. Withayachumnankul, S. F. Al-Sarawi and D. Abbott, "Metamaterial-Inspired Rotation Sensor With Wide Dynamic Range," *IEEE Sensors J.*, vol. 14, no. 8, pp. 2609-2614, Aug. 2014.

[19] J. Naqui, J. Coromina, A. Karami-Horestani, C. Fumeaux, and F. Martín, "Angular displacement and velocity sensors based on coplanar waveguides (CPWs) loaded with S-shaped split ring resonator (S-SRR)," *Sensors*, vol. 15, pp. 9628–9650, 2015.

[20] A. K. Horestani, J. Naqui, Z. Shaterian, D. Abbott, C. Fumeaux, and F. Martín, "Two-dimensional alignment and displacement sensor based on movable broadside-coupled split ring resonators," *Sensors and Actuators A*, vol. 210, pp. 18–24, April 2014.

[21] J. Naqui, *et al.*, "Transmission lines loaded with pairs of magnetically coupled stepped impedance resonators (SIRs): modeling and application to microwave sensors," *IEEE MTT-S Int. Microwave Symp.*, Tampa, FL, USA, June 2014, pp. 1–4.

[22] L. Su, J. Naqui, J. Mata-Contreras, and F. Martín "Modeling metamaterial transmission lines loaded with pairs of coupled split ring resonators," *IEEE Ant. Wireless Propag. Lett.*, vol. 14, pp. 68–71, 2015.

[23] L. Su, J. Naqui, J. Mata-Contreras, and F. Martín, "Modeling and applications of metamaterial transmission lines loaded with pairs of coupled complementary split ring resonators (CSRRs)," *IEEE Ant. Wireless Propag. Lett.*, vol. 15, pp. 154–157, 2016.

[24] L. Su, J. Mata-Contreras, J. Naqui, and F. Martín, "Splitter/combiner microstrip sections loaded with pairs of complementary split ring resonators (CSRRs): modeling and optimization for differential sensing applications," *IEEE Trans. Microw. Theory Techn.*, vol. 64, pp. 4362-4370, Dec. 2016.

[25] A. Ebrahimi, J. Scott and K. Ghorbani, "Differential sensors using microstrip lines loaded with two split ring resonators," *IEEE Sensors J.*, vol. 18, pp. 5786-5793, Jul. 2018.

[26] P. Vélez, L. Su, K. Grenier, J. Mata-Contreras, D. Dubuc, and F. Martín, "Microwave microfluidic sensor based on a microstrip splitter/combiner configuration and split ring resonators (SRR) for dielectric characterization of liquids", *IEEE Sensors J.*, vol. 17, pp. 6589-6598, Oct. 2017.

[27] C. Damm, *et al.*, "Artificial transmission lines for high sensitive microwave sensors," *IEEE Sensors Conf.*, Christchurch, New Zealand, 2009, pp. 755–758.

[28] F.J. Ferrández-Pastor, J.M. García-Chamizo and M. Nieto-Hidalgo, "Electromagnetic differential measuring method: application in microstrip sensors developing", *Sensors*, vol. 17, p. 1650, 2017.

[29] P. Vélez, K. Grenier, J. Mata-Contreras, D. Dubuc, and F. Martín, "Highly-sensitive microwave sensors based on open complementary split ring resonators (OCSRRs) for dielectric characterization and solute concentration measurements in liquids", *IEEE Access*, vol. 6, pp. 48324-48338, Dec. 2018.

[30] P. Vélez, J. Muñoz-Enano, K. Grenier, J. Mata-Contreras, D. Dubuc, F. Martín, "Split ring resonator (SRR) based microwave fluidic sensor for electrolyte concentration measurements", *IEEE Sensors J.*, vol. 19, no. 7, pp. 2562-2569, Apr. 2019.

[31] D.M. Pozar, *Microwave Engineering*, 4th Ed., Wiley, Hoboken, NJ, 2011.

[32] A. Ebrahimi, J. Scott and K. Ghorbani, "Transmission Lines Terminated With LC Resonators for Differential Permittivity Sensing," in IEEE

Microwave and Wireless Components Letters, vol. 28, no. 12, pp. 1149-1151, Dec. 2018.

[33] A. Ebrahimi, A. Ahmed, B. Mapleback, J. Scott and K. Ghorbani, "Microstrip lines loaded with bandstop resonators for high resolution permittivity sensing," *2018 Asia-Pacific Microw. Conf.* (APMC), Kyoto, 2018, pp. 926-928.

[34] J. Naqui, C. Damm, A. Wiens, R. Jakoby, L. Su, J. Mata-Contreras, F. Martín, "Transmission lines loaded with pairs of stepped impedance resonators: modeling and application to differential permittivity measurements", *IEEE Trans. Microw. Theory Techn*., vol. 64, no. 11, pp. 3864-3877, Nov. 2016.

[35] D. Isakov, C. J. Stevens, F. Castles and P. S. Grant, ""A split ring resonator dielectric probe for near-field dielectric imaging", *Sci. Rep.*, vol. 7, article number 2038, 2017.

[36] N. M. Shebani, B. M. Khamoudi, and A. S. Abul-kassem, "Measurement of Dielectric Constant of Some Materials Using Planar Technology", *Second Int. Conf. on Comp. and Electrical Engineering*, Dubai, United Arab Emirates, Dec. 2009, pp. 352-356.

[37] D. Shimin, "A new method for measuring dielectric constant using the resonant frequency of a patch antenna, "*IEEE Trans. Microw. Theory Tech*., vol. 34, no. 9, pp. 923–931, Sep. 1996.

[38] P. Vélez, J. Muñoz-Enano, M. Gil, J. Mata-Contreras, and F. Martín, "Differential Microfluidic Sensors Based on Dumbbell-Shaped Defect Ground Structures in Microstrip Technology: Analysis, Optimization, and Applications", *Sensors*, vol. 2019, pp. 1-18, July 2019.

Jonathan Muñoz-Enano (GS'19) was born in Mollet del Vallès (Barcelona), Spain, in 1994. He received the Bachelor's Degree in Electronic Telecommunications Engineering in 2016 and the Master's Degree in Telecommunications Engineering in 2018, both at the Autonomous University of Barcelona (UAB). Actually, he is working in the same university in the elaboration of his PhD, which is focused on the development of microwave sensors based on metamaterials concepts for the dielectric characterization of materials and biosensors.

Paris Vélez (S'10–M'14) was born in Barcelona, Spain, in 1982. He received the degree in Telecommunications Engineering, specializing in electronics, the Electronics Engineering degree, and the Ph.D. degree in Electrical Engineering from the Universitat Autònoma de Barcelona, Barcelona, in 2008, 2010, and 2014, respectively. His Ph.D. thesis concerned common mode suppression differential microwave circuits based on metamaterial concepts and semi-lumped resonators. During the Ph.D., he was awarded with a pre-doctoral teaching and research fellowship by the Spanish Government from 2011 to 2014. From 2015-2017, he was involved in the subjects related to metamaterials sensors for fluidics detection and characterization at LAAS-CNRS through a TECNIOSpring fellowship cofounded by the Marie Curie program. His current research interests include the miniaturization of passive circuits RF/microwave and sensors-based metamaterials through Juan de la Cierva fellowship. Dr. Vélez is a Reviewer for the IEEE Transactions on Microwave Theory and Techniques and for other journals.

Marta Gil Barba (S'05-M'09) was born in Valdepeñas, Ciudad Real, Spain, in 1981. She received the Physics degree from Universidad de Granada, Spain, in 2005, and the Ph.D. degree in electronic engineering from the Universitat Autònoma de Barcelona, Barcelona, Spain, in 2009. She studied one year with the Friedrich Schiller Universität Jena, Jena, Germany. During her PhD Thesis she was holder of a METAMORPHOSE NoE grant and National Research Fellowship from the FPU Program of the Education and Science Spanish Ministry. As a postdoctoral researcher, she was awarded with a Juan de la Cierva fellowship working in the Universidad de Castilla-La Mancha. She was postdoctoral researcher in the Institut für Mikrowellentechnik und Photonik in Technische Universität Darmstadt and in the Carlos III University of Madrid. She is currently assistant professor in the Universidad Politécnica de Madrid. She has worked in metamaterials, piezoelectric MEMS and microwave passive devices. Her current interests include metamaterials sensors for fluidic detection.

Ferran Martín (M'04-SM'08-F'12) was born in Barakaldo (Vizcaya), Spain in 1965. He received the B.S. Degree in Physics from the Universitat Autònoma de Barcelona (UAB) in 1988 and the PhD degree in 1992. From 1994 up to 2006 he was Associate Professor in Electronics at the Departament d'Enginyeria Electrònica (Universitat Autònoma de Barcelona), and since 2007 he is Full Professor of Electronics. In recent years, he has been involved in different research activities including modelling and simulation of electron devices for high frequency applications, millimeter wave and THz generation systems, and the application of electromagnetic bandgaps to microwave and millimeter wave circuits. He is now very active in the field of metamaterials and their application to the miniaturization and optimization of microwave circuits and antennas. Other topics of interest include microwave sensors and RFID systems, with special emphasis on the development of high data capacity chipless-RFID tags. He is the head of the Microwave Engineering, Metamaterials and Antennas Group (GEMMA Group) at UAB, and director of CIMITEC, a research Center on Metamaterials supported by TECNIO (Generalitat de Catalunya). He has organized several international events related to metamaterials and related topics, including Workshops at the IEEE International Microwave Symposium (years 2005 and 2007) and European Microwave Conference (2009, 2015 and 2017), and the Fifth International Congress on Advanced Electromagnetic Materials in Microwaves and Optics (Metamaterials 2011), where he has acted as chair of the Local Organizing Committee. He has acted as Guest Editor for five Special Issues on Metamaterials and Sensors in five International Journals. He has authored and co-authored over 550 technical conference, letter, journal papers and book chapters, he is co-author of the book on Metamaterials entitled *Metamaterials with Negative Parameters: Theory, Design and Microwave Applications* (John Wiley & Sons Inc.), author of the book *Artificial Transmission Lines for RF and Microwave Applications* (John Wiley & Sons Inc.), and co-editor of the book *Balanced Microwave Filters* (John Wiley & Sons Inc.). Ferran Martín has generated 19 PhDs, has filed several patents on metamaterials and has headed several Development Contracts.

Prof. Martín is a member of the IEEE Microwave Theory and Techniques Society (IEEE MTT-S). He is reviewer of the IEEE Transactions on Microwave Theory and Techniques and IEEE Microwave and Wireless Components Letters, among many other journals, and he serves as member of the Editorial Board of IET Microwaves, Antennas and Propagation, International Journal of RF and Microwave Computer-Aided Engineering, and Sensors. He is also a member of the Technical Committees of the European Microwave Conference (EuMC) and International Congress on Advanced Electromagnetic Materials in Microwaves and Optics (Metamaterials). Among his distinctions, Ferran Martín has received the 2006 Duran Farell Prize for Technological Research, he holds the *Parc de Recerca UAB – Santander* Technology Transfer Chair, and he has been the recipient of three ICREA ACADEMIA Awards (calls 2008, 2013 and 2018). He is Fellow of the IEEE and IET.